Energy Conversion and Management 288 (2023) 117123

Contents lists available at ScienceDirect

Energy Conversion and Management

journal homepage: www.elsevier.com/locate/enconman

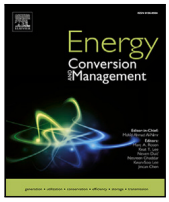

Thermo-economic analysis of a low-cost greenhouse thermal solar plant with seasonal energy storage

A. Tafuni [a], A. Giannotta [a,*], M. Mersch [b], A.M. Pantaleo [b], R. Amirante [a], C.N. Markides [b], P. De Palma [a]

[a] Department of Mechanics, Mathematics and Management, Politecnico di Bari, via Re David, 200, Bari, 70125, Italy
[b] Clean Energy Process (CEP) Laboratory, Department of Chemical Engineering, Imperial College, South Kensington Campus, SW7 2AZ, London, UK

ARTICLE INFO

Keywords:
Thermal storage
Dual-media
Greenhouse

ABSTRACT

Reduction of greenhouse gas emissions is today mandatory to limit the increase of ambient temperature. This paper provides a numerical study of a thermal solar plant using a seasonal dual-media sensible heat thermal energy storage system for supplying the total energy demand of a greenhouse located in the South of Italy, avoiding the use of the gas boiler. The aim of the work is to assess the technical and economic performance of a low-cost pit storage system, made of gravel and water, placed under the greenhouse to save surface. The study provides an original analysis of the charging and discharging phases during one year of operation on the basis of the real hourly heating demand and on real weather data. A sensitivity analysis of the levelized cost of heat is carried on with respect to the solar-collector area and to the storage-pit volume. The analysis shows that a minimum-cost design solution exists to cover 100% of the heat demand with an estimated levelized cost of heat of 153.3 EUR/MWh. The results demonstrate that dual-media thermal energy storage systems with solar thermal collectors represent a viable solution for reducing the environmental impact of greenhouses.

1. Introduction

Global climate warming due to greenhouse gas emissions is pushing human society to change the paradigm of energy production in favor of clean technologies harvesting solar and wind energy [1]. Such technologies may be employed to satisfy both the final demand for electricity and heat. The International Energy Agency (IEA) reported that global energy demand is increased by 4.6% in 2021, more than offsetting the 4% contraction in 2020 and pushing the demand 0.5% above 2019 levels [2]. Primary energy demand is set to increase in the "stated policy scenario" by about 1% a year to 2030, which should be largely met through increased use of renewables. Instead, in the "announced pledges scenario", the energy demand is set to increase by 0.2% a year to 2030 [3]. The REPowerEU plan, published in May 2022, revises the EU target for renewables setting the total final consumption share to 45% by 2030, with the aim of achieving at least 55% greenhouse gas (GHG) emissions reductions by 2030.

Heat is the largest energy final use, representing about 50% of global final energy consumption, contributing to about 39% of the global energy-related carbon dioxide emissions [1]. In 2020, after several years of steady decrease, the total share of coal, oil and natural gas employed in boilers for heating equipment fell under 50%. The overall energy system is slowly transitioning from a fossil fuel-dominated technology mix towards more sustainable and renewable solutions. Plants using heat pumps and renewable heating equipment, such as solar hot water systems, achieved about 20% of overall installations in 2020. Nevertheless, these data are still very far from the "Net Zero Emissions by 2050" scenario, in which the share of heat pumps, low-carbon district heating and renewables-based heating should exceed 80% of sales in 2030 [4], the share of renewables (excluding traditional biomass) in global heat consumption being only 11% in 2021, almost unchanged from the previous year [1]. About 53% of total heat produced is used for industrial processes, and about 44% is consumed in buildings for space and water heating and for cooking (in a minor part), while the remainder is employed in agriculture, especially for greenhouse heating. The heating demand is largely satisfied by fossil fuels, with renewable energy sources meeting less than one-quarter of global heat demand in 2021 (including traditional biomass, which makes up about half of this amount) [1]. In the "net zero emissions" scenario [5], the direct use of modern renewable energy should rise from about 10% of the global heating demand in 2020 to 40% in 2050, about three-quarters of the increase coming from solar thermal and geothermal. In September 2022, the European Parliament adopted a series of amendments that define its starting position for the ongoing

* Corresponding author.
E-mail address: alessandro.giannotta@poliba.it (A. Giannotta).

https://doi.org/10.1016/j.enconman.2023.117123

Available online 16 May 2023

negotiations on the Renewable Energy Directive II revision proposal. They propose the indicative target of a 2.3-percentage-point average annual increase in the share of renewables in heating and cooling during the periods 2021–2025 and 2026–2030 and the same target for district heating and cooling; an indicative average annual increase of 1.9 percentage points in industry during the periods 2024–2027 and 2027–2030; and an indicative target of 49% renewables in buildings by 2030. This is a very tough challenge considering that over 2010–2020, the EU share of renewables in heating and cooling increased by just 0.6 percentage points annually on average, with the industry sector on its own performing similarly.

However, there is one obstacle hampering the use of solar energy for space heating, namely the phase shift between solar energy availability and energy demand. One solution to such a problem, on a large time scale of about one year, is the use of seasonal thermal energy storage (STES) systems, allowing solar energy captured during the summer months to be stored and then employed during the winter months, when heating demand grows. Therefore, expanding the set of energy storage technologies and addressing emerging needs for long-duration seasonal storage is very important. Research efforts on such issues would be useful to support the stability of power grids with high shares of solar and wind energy contributions [5]. The present work focuses on the analysis of a solar field for satisfying the heat demand of a greenhouse. Greenhouses are enclosed structures trapping solar radiation to create a suitable micro-climate for higher crop productivity [6]. Therefore, unlike conventional buildings, greenhouses are designed to maximize the incoming solar radiation. This is achieved by using cover materials with low-insulating properties. As a consequence, depending on climate conditions, significant heating energy could be needed during winter months, summing up to 90% of the annual greenhouse energy demand [7].

Today, energy consumption in greenhouses represents a challenging issue due to the rise of energy costs and to environmental impact deriving from the use of fossil energy sources. Conventional greenhouses have a large amount of energy required per crop yield (specific energy utilization). The cost of energy can achieve 50% of the production cost [8]. Clean energy sources could represent the solution to both problems of costs and GHG emissions [9]. In particular, recently, renewable solar energy has shown a good potential of integration with greenhouse structures, contributing to the reduction of GHG emissions [10]. Solar energy technologies can be categorized as solar thermal and photovoltaic (PV). Solar thermal plants convert solar-radiation energy into heat by flat-plate or concentrating solar collectors. The energy can be stored as sensible heat of some material and employed when needed [11]. On the other hand, PV systems employ semiconductors, to convert sunlight into electricity. Both thermal and PV technologies are employed in greenhouses. The integration of renewable energy sources with greenhouses, including solar thermal and PV, Photovoltaic-Thermal (PVT), geothermal energy, and biomass, have been broadly investigated in literature. In particular, Gorjian et al. [12] reviews the combined use of renewable resources and various TES systems for greenhouses, including economic aspects of net zero configurations and their associated environmental impacts. The present work focuses on the use of solar thermal plants [13]. Solar thermal systems represent an interesting technology for their high energy conversion efficiency and energy storage density [14]. They consist of two main components, namely, the solar collector and the thermal energy storage (TES) unit. In greenhouse applications, thermal collectors are used to absorb solar radiation and produce heat which can then be transferred to the indoor space of the greenhouse to provide an optimum thermal environment for plants cultivated inside [15]. The collected thermal energy, not directly employed in the indoor space of the greenhouse, can be stored in a suitable material to be employed during nocturnal periods, cloudy days, or during the winter period (seasonal storage) [16]. Solar thermal collectors are categorized into non-concentrating and concentrating types [8]. In particular, the present work focuses on a low-cost non-concentrating solar collector coupled with a sensible-heat thermal energy storage (SHTES) system. Such systems have been widely considered due to their simplicity and reliability. SHTES materials, generally solid or liquid, should be easy to find avoiding processing and manufacturing (water, sand, rock, etc.). Therefore, a very efficient low-cost storage system can be designed [17]. Solid materials, such as metals, bricks, concrete, graphite, rocks, and salts, can be employed for low and high temperatures. The properties of the materials and the porosity of the system can be chosen to obtain the desired thermal energy storage capacity and system charging time with a simple arrangement, which can withstand high mechanical loads and is free of leakage. Liquid materials, such as water, oil and molten salt, are also commonly used for SHTES. Obviously, for low temperatures, water is one of the best storage materials due to its high specific heat and low cost [18]. Rock-bed thermal storage systems for a greenhouse coupled to a solar plant were proposed in [19] and in [20] and for night-day balance of heating demand and solar input supply, with the storage bed located on the ground, and reporting an improvement of cultivation yield of around 22%. A comprehensive review of water based thermal storage solutions for solar driven energy systems is provided in [21], with a specific focus on water tanks, pits, aquifers, caverns, and addressing the issues of thermal insulation materials, coupling with solar harvesting systems, but not including water-gravel storage options. An overview of thermal energy storage solutions for closed greenhouses without ventilation is also proposed in [22], comparing from a techno-economic point of view underground thermal energy storage, stratified chilled water storage and phase change material storage for daily demands and peak loads coverage, while [23] includes also aquifers, borehole or cavers, and solutions for cooling and moisture control. In the same work, relevant case studies for thermal energy storage in greenhouses are proposed. In [24], a solar thermal heating system with underground storage for a greenhouse in Tunisia was modeled using Transys. The optimal solar collector and thermal storage sizing was assessed in [25] for a night heating of a greenhouse with solar thermal collectors and water tanks, calibrating and validating a tank temperature model capable to predict water temperatures in the storage tank with an average accuracy of 0.4 °C, resulting in greenhouses ground area around 4.5 times higher than the solar collectors surface to maintain temperatures above 12 °C under Beijing climate conditions. To facilitate a 1 °C increase in the air temperature set-point, approximately 2 m^2 of additional solar collectors and 0.1 m^3 of additional storage tanks were also needed. Different solutions with fully or half removable back walls were considered in [26] to improve the thermal performance of conventional single span greenhouses. Hybrid SHTES can be designed by adding solid materials (e.g., pebbles) into water [27]. Alptekin and Ezan [28] have studied numerically the performance of a solar hybrid SHTES made by water and spherical quartzite rock. They could fulfill the low-temperature heating demands of a building based on four-month real weather data by achieving a temperature range of 40–60 °C. Lugolole et al. [29] provided an experimental study of the discharge phase of SHTES systems made by sun-flower oil and granite rock with different pebble sizes. They showed that the discharging performance of the hybrid system improved with respect to the liquid TES. Schmidt et al. [30] studied a hybrid seasonal solar energy storage system made by gravel and water. In this case, another advantage of the hybrid system was exploited, namely, the gravel structure's capacity to withstand a weight load. Concerning recent works focused on the use of thermal solar collectors in greenhouses, Kim et al. [31] studied, by an experimental analysis, the economic benefits of solar thermal and seasonal thermal energy storage for greenhouses. They considered a system composed of solar collectors, seasonal thermal energy storage, hybrid-source heat pumps, and ground-source heat pumps. The authors demonstrate that operating cost savings and greenhouse gas emission reductions of the proposed system were 73% and 82%, respectively, with respect to those

of conventional systems based on fossil fuel. They estimated a pay-back period of about 25 years without considering carbon credits.

All these studies have shown that the introduction of solar-based heating systems is a promising strategy to decarbonize the greenhouse sector, today based on extensive utilization of fossil fuels. However, because solar energy fluctuates on seasonal and hourly time scales, large-scale seasonal (TES) systems must be employed, which need a careful design in order to reduce investment costs. For this purpose, numerical models can be fundamental in the design process. As stated by Tosatto et al. [32], TES modeling can be performed at different levels, namely, at system-level, at component-level and at hydrogeological-level, depending on the required outputs and on the considered control volume and available boundary conditions. Dahash et al. [33] have developed a numerical finite element approach to simulate the operation of large-scale tanks and pits. The models have been validated versus measured data from the Dronninglund pit TES in Denmark. The results have demonstrated the accuracy of the numerical approach, highlighting the fundamental role of the calibration of the model parameters with respect to the specific real operating conditions. The work of Dahash et al. [33] is an example of component-level study of the storage system including the geometrical details of the construction and the ground model, which is necessary for environmental impact assessments. Tosatto et al. [32] extend the detailed model to the study of the influence of the use of heat pumps in conjunction with large-scale thermal energy storage systems for district heating. On the other hand, very few articles can be found in the literature addressing the hourly-based operation optimization of an entire solar energy plant, including seasonal heat storage, to cover greenhouse energy demand. Indeed, the hourly operation of this energy system for a whole year is essential since the greenhouse heating load has a significant seasonal effect. Semple et al. [6] studied the use of a large-scale solar collector system in combination with seasonal heat storage for heating a large greenhouse. In particular, this study provided a model for the borehole thermal energy storage system and proved the feasibility of the system to cover up to 65% of the greenhouse heating demand, reduce the annual carbon dioxide equivalent emissions by about 220 t/Acre. Recently, Mohebi and Roshandel [34] have proposed a novel method based on a linear methodology for optimizing the design and hourly operation of an entire plant consisting of a hybrid solar energy system with gas boiler and with seasonal and short-term heat storage systems, that meets the hourly heating demand of a greenhouse for an entire year. They also evaluated the impact of the dynamic greenhouse heating demand on the optimal energy system under different growing seasons.

The present work focuses on the system-level modeling approach aiming at simulating an entire solar plant for greenhouse heating, allowing an evaluation of the role of the thermal energy storage within the system, its integration within the plant, and the choice of the optimal size of the TES and of the collector field minimizing the levelized cost of heat while satisfying 100% of the heat demand. The work is based on a numerical approach with the following hypothesis: (i) a dual-media sensible heat thermal energy storage (DM-SHTES) system is considered; (ii) a one-dimensional model of the DM-SHTES system is adopted to study the temperature stratification; (iii) a one-dimensional model of the heat exchanger is considered to join the solar collector field with the DM-SHTES. The aim of this work is to design and evaluate the efficiency of a low-cost seasonal pit storage system, made of gravel and water, to be installed under the greenhouse in order to save space. The SHTES system is coupled with a thermal solar field, made of flat plate solar collectors, designed to cover the total annual heating demand of the greenhouse. This study provides an original analysis of the charging and discharging phases during one year of operation on the base of the real hourly heating demand data of a greenhouse located in the South of Italy (Bari) and on real hourly weather data. The present work represents, to the authors' knowledge, one of the first studies of DM-SHTES systems for greenhouse applications performing time-dependent simulations over a one-year time scale with an assessment of the economic return and environmental impact of the plant. The paper is organized as follows: Section 1 provides a description of the plant and the measured data. Section 2 describes the modeling method, discussing the details of each component of the plant and their interactions. Section 3 provides the details of the economic model employed to estimate the costs of the plant and the levelized cost of heat. The results of the simulation are discussed in Section 4 and, finally, the conclusions of the work are drawn in Section 5.

2. Description of the plant

In the present work, a 10800 m^2 greenhouse located in Bari, Italy is considered, where the local mean annual insolation reaches about 6120 MJ/m^2. As shown in Fig. 1, the considered plant is composed of four main parts: (1) the greenhouse (GH); (2) the flat-plate solar collector (SC) field; (3) the brazed-plate heat exchanger (HEX); (4) the seasonal thermal energy storage (TES).

In the SC, the solar radiance is absorbed by the receivers for generating a hot fluid. The thermal energy provided by the solar collectors is then stored in the seasonal thermal energy storage. Finally, the thermal energy for the greenhouse is provided by the TES system, also during months with low insolation. The measured annual distribution in 2016 of the solar irradiance (I_m) and ambient temperature at the location of the considered greenhouse are shown in Figs. 2 and 3, respectively. The greenhouse is employed for tomatoes production and it has the necessity to maintain the air temperature in the range 13 °C–40 °C, as shown in Fig. 4. The heat demand data of the greenhouse in the year 2016 is available, the overall annual thermal energy demand being 809 MWh, which is supplied by a boiler gas plant. In particular, a natural-gas-fired hot water generator is used in the current energy infrastructure to fulfill the thermal energy demand and the hot water is distributed throughout the greenhouse in a closed loop with air heat exchangers. Available data supplied by the farm operator includes quarterly-hour heat consumption data.

The aim of this work is therefore to study an innovative and market-competitive renewable energy system to fulfill the total heat energy demand. The system consists of combining a field of solar thermal collectors with a thermal energy storage system. The main challenge is to develop an efficient and economically competitive TES, considering a dual-media thermal storage solution and optimizing the system by means of theoretical models and numerical simulations on the base of real data concerning the heat demand time distribution. The TES under consideration is a seasonal dual-media (water and gravel) TES. Heat is charged into the TES by means of a circuit at a high temperature linked to the solar collector field. A heat exchanger is placed between the SC and the TES, because the water flowing in the SC is usually mixed with additives and cannot be delivered to the TES. On the discharging side, water from the TES is directly circulated in the greenhouse since no additives are employed. Temperature stratification is supported by the charging device with a suitable choice of the TES volume.

3. Modelling method

In the present section, a description of the models employed for each component of the plant described above is provided.

3.1. Greenhouse model

The model of the energy plant is based on real data regarding the thermal power load required by the greenhouse hour by hour during one year of operation. In particular, the measured time distribution of the real heating load, $Q_{in}(t)$ reported in Fig. 5 is necessary to guarantee the air temperature inside the greenhouse, $T_{air,GH}(t)$ given in Fig. 4.

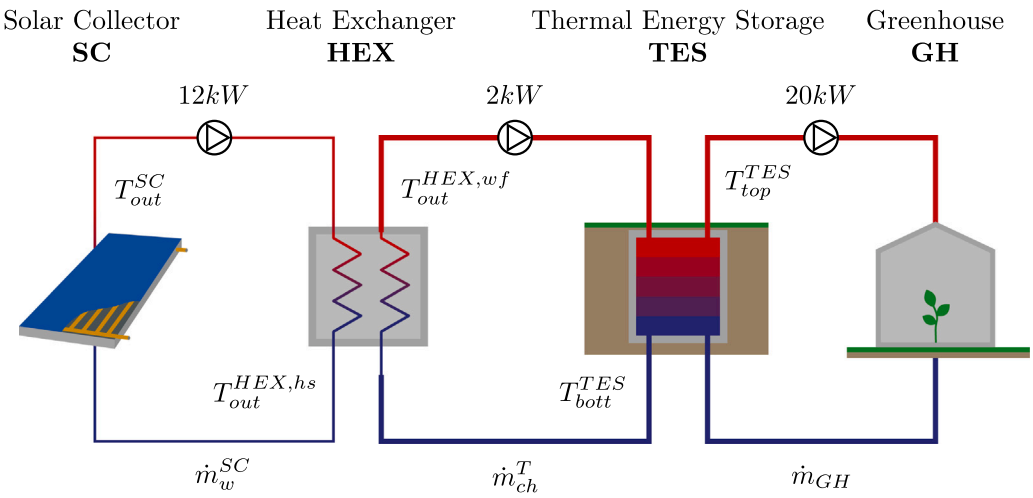

Fig. 1. Plant diagram.

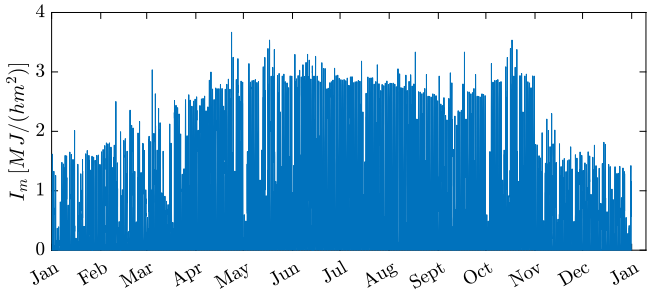

Fig. 2. Measured solar irradiance.

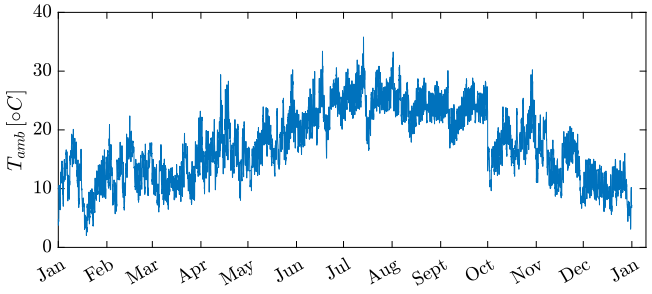

Fig. 3. Measured ambient temperature.

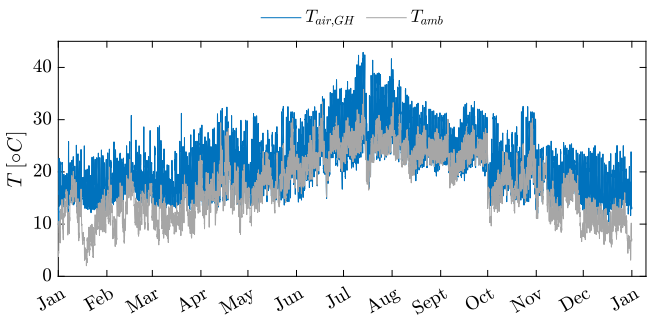

Fig. 4. Measured greenhouse air temperature (blue line). The gray line indicates the ambient temperature.

The value of the temperature of the water circulating in the heating system at the exit from the greenhouse is set to $T_{w,out} = 40$ °C. Then, given the values of $\dot{Q}_{in}$ and of the inlet temperature of the water coming from the TES, $T_{w,in}$, it is possible to calculate the water mass flow rate through the greenhouse heating system, $\dot{m}_{GH}$, by the following energy balance equation

$$\dot{Q}_{in} = \dot{m}_{GH}\, c_f\, (T_{w,in} - T_{w,out}), \tag{1}$$

where c_f is the specific heat of water.

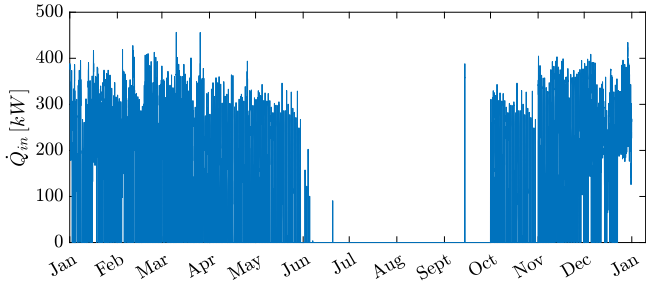

Fig. 5. Measured greenhouse heating load.

3.2. Solar collector model

The solar collector model employs the classical quadratic efficiency equation based on the ratio of the collector-to-ambient temperature difference, $T_m^{SC} - T_{amb}$, and the incident solar irradiation, I_i,

$$\eta = \eta_0 - \frac{a_1\,(T_m^{SC} - T_{amb})}{I_i} - \frac{a_2\,(T_m^{SC} - T_{amb})^2}{I_i}, \tag{2}$$

where T_m^{SC} is the collector temperature, computed as the average between the inlet water temperature, T_{in}^{SC}, and the outlet temperature, T_{out}^{SC}; T_{amb} is the ambient temperature; I_i is the global solar irradiance incident on the collector. The optical efficiency, $\eta_0 = 0.77$, as well as the linear, $a_1 = 3.45$ W/(Km^2), and quadratic, $a_2 = 0.0083$ W/(K^{2}m^2) heat loss coefficients, are taken from collector data sheets and correspond to low-cost solar thermal collector [35]. A quadratic model has been adopted with two coefficients because it is known to provide a more accurate prediction of the collector efficiency at higher operating temperatures and it represents a good compromise, for the present application, with respect to more complex models. The model assumes collectors to be installed at a tilt angle of 32° facing to the south, which is the optimal orientation of the location of the present application and should be adapted for different latitudes.

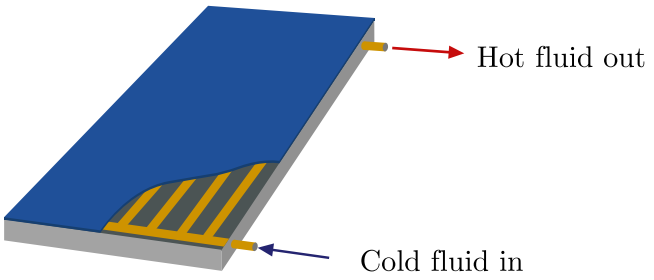

Fig. 6. Solar collector.

The global incident irradiance has to be estimated from the measured global irradiance, I_m. For this purpose, the measured irradiance is decomposed in the direct-irradiance contribution (I_{direct}) plus a diffusion contribution (I_{diff}) and the incident irradiance on the collector is computed as [36]

$$I_i = I_{direct}\cos(\theta) + I_{diff}, \tag{3}$$

where θ is the incidence angle between the solar beam and the normal to the collector surface [37]. The decomposition of I_m is obtained by firstly computing the clearness index as

$$k_t = \frac{I_m}{I_{clear}}, \quad I_{clear} = I_{ext}\cos(z), \tag{4}$$

where I_{ext} is the extraterrestrial radiation computed by the Maxwell approach [38] and z is the solar zenith angle. Then, using the value of k_t and the one-predictor equation of Ridley et al. [39], the diffusive fraction of the irradiance, $d = I_{diff}/I_m$, is evaluated as

$$d = \frac{1}{1+\exp -5.0033 + 8.6025\,k_t}. \tag{5}$$

Finally, the direct radiation is estimated as

$$I_{direct} = I_m - I_{diff} \tag{6}$$

and Eq. (3) is applied to compute I_i.

The model employs the following energy balance equation of the solar collector:

$$\dot{Q}_{SC} = \eta\ I_i\ A_{SC}, \tag{7}$$

where A_{SC} is the total area of the solar collector field; the thermal power term in the above equation is written as

$$\dot{Q}_{SC} = c_f^{SC}\ \dot{m}_w^{SC}\ (T_{out}^{SC} - T_{in}^{SC}), \tag{8}$$

where c_f^{SC} and $\dot{m}_w^{SC}$ are the specific heat and the mass flow rate of the fluid flowing in the solar collector (see Fig. 6), respectively.

It is assumed that the solar collector field had a series-parallel arrangement. The flow rate through the solar collectors is set at 12.5 kg/(hm^2) for a temperature rise through the solar collectors $\Delta T^{SC} \leq$ 15 K and is increased to 25 kg/(hm^2) when $\Delta T^{SC} >$ 15 K. From Eq. (8), T_{out}^{SC} is then computed. The solar collector load and the corresponding circulating pumps are turned on when $\Delta T^{SC} \geq$ 6 K.

3.3. Heat exchanger model

A brazed plate counter-flow heat exchanger has been modeled to compute the heat exchange between the solar system and the TES [40]. It is assumed that the mass flows are equally divided between the channels of the HEX and that no losses occur at the inlet and outlet. A 50% propylene-glycol to water mixture is employed for the solar collector pipe loop having a specific heat capacity of 3.6 kJ/(kgK) at 313 K [6]. Water is used as heat sink fluid (TES charging circuit) on the load side of the heat exchanger. The heat source and sink are assumed to be at atmospheric pressure. The flow rate of the sink fluid through the heat exchanger, $\dot{m}_{ch}^{T}$, is computed in order to obtain the same effective capacitance of the hot-flow side. The heat exchanger models have four geometric degrees of freedom: The length and width of the plates, the plate spacing and the number of plates. The HEX behavior depends on the working fluid flow regime. In the present case, a single-phase fluid flows through the source and sink sides of the exchanger. The HEX is discretized into one-dimensional cells based on equal temperature increments. All fluid properties in each cell are assumed to be equal to the mean of the values at the extreme points. For each cell "i", the heat transfer coefficient (HTC), U_i, is determined as:

$$\frac{1}{U_i} = \frac{1}{h_{so,i}} + \frac{s}{k} + \frac{1}{h_{si,i}}, \tag{9}$$

where k represents the thermal conductivity of the wall, s is the wall thickness, $h_{so,i}$ and $h_{si,i}$ are the heat transfer coefficients of the source and sink flows, respectively. Notice that, in the present work, a simplified model for the HEX has been considered, neglecting the increase of the thermal resistance of the heat exchanger and its thermal degradation due to fouling. The Nusselt number (Nu), employed to compute the HTCs, is expressed as a function of the Reynolds (Re) and Prandtl (Pr) numbers:

$$Nu = aRe^b Pr^c, \tag{10}$$

where a, b, and c are model coefficients given by the correlations of Bogaert and Böles [41], for Reynolds numbers lower than 1000, and Chisholm and Wanniarachchi [42], for higher Reynolds numbers. The heat flux rate for each (source/sink) cell is computed as:

$$Q_i = U_i A_i \Delta T_{ln,i}, \tag{11}$$

where, A_i is the heat transfer surface and $\Delta T_{\ln,i}$ is the log-mean temperature difference between source (SC) and sink (TES) flows. The computed heat flux rates are used to determine the heat source/sink fluid temperature at each node. In the present computations, the HEX has been discretized using five cells as a compromise between accuracy and computational speed. The HEX calculations are an iterative process. The simulation model requires a first estimate of the working fluid outlet temperature. A temperature difference of 5 K at the HEX outlet with respect to the inlet value is used as an initial guess. A tolerance of 0.5 K is employed to stop the iterative procedure.

The total area of the HEX, equal to 30 m^2, is determined with respect to the average power of the solar field and the expected temperature variations through the exchanger. The main geometrical parameters considered in the brazed-plate HEX model are reported in Table 1.

Table 1
Data for HEX simulation.

Parameter	Unit	Value
Base surface	m^2	30
N. of channels working fluid	–	9
N. of channels heat source fluid	–	10
Plate spacing	m	1.5E−02
Channel width	m	0.1
Chevron angle	deg	45
Plate thickness	m	1.5E−04
Thermal conductivity of plate material (copper)	W/(mK)	385

3.4. Thermal energy storage model

The proposed plant includes a seasonal thermal energy storage system consisting of a water/gravel pit. A multi-physics model has been implemented in order to predict the thermo-hydraulic behavior of the TES, estimating conductive heat transfer, convective heat transfer, and energy fluxes due to mass transfer.

The model simulates a cylindrical storage pit discretized by a one-dimensional mesh in the vertical direction in order to capture the

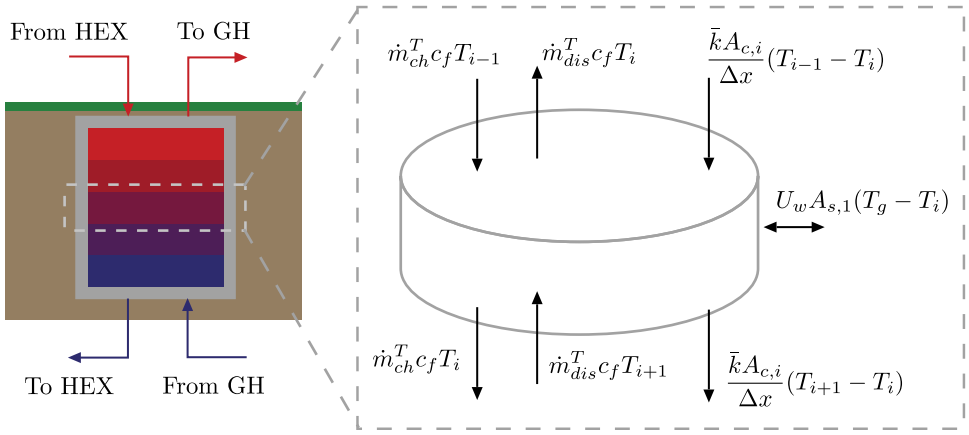

Fig. 7. TES 1-D model.

thermal stratification. The unsteady energy balance equation for each cell "i" of the mesh reads

$$\frac{\partial E_i(t)}{\partial t} = \dot{m}^T_{ch}(h_{ch,in} - h_{ch,out})_i + \dot{m}^T_{dis}(h_{dis,in} - h_{dis,out})_i + \left(\dot{Q}_{in} - \dot{Q}_{out}\right)_i - \dot{Q}_{loss,i}, \tag{12}$$

where the first two terms at the r. h. s. represent the enthalpy fluxes, $\dot{m}^T_{ch}$ and $\dot{m}^T_{dis}$ being the mass flow rate of water flowing in the charging (HEX side) and discharging (GH side) pipes, respectively. The third term is the conductive heat transfer between adjacent cells, and the last term represents the thermal losses. The TES volume is assumed to contain concrete gravel and to be isolated from the surrounding ground by a water-proof surface composed of three layers of HDPE polymembrane, ALU foil and Geotextile, respectively. Fan et al. [43] have modeled the characteristics of this wall and, by matching the experimental data from the real pit, have obtained a heat transfer coefficient to the ground of $U_w = 0.2$ W/(m^{2}K). The tank is divided into N fully mixed equal volume cells, having height Δx, transversal area $A_{c,i}$, external area $A_{s,i}$, mass m_i and constant temperature, T_i, as shown in Fig. 7. A dual-media storage system is adopted, composed of a liquid fluid (water) and a solid material (gravel). The discretized form of the energy balance equation for cell "i" reads

$$m_i \bar{c} \frac{T_i^{n+1} - T_i^n}{\Delta t} = \dot{m}^T_{ch} c_f (T_{i-1} - T_i) + \dot{m}^T_{dis} c_f (T_{i+1} - T_i) + \bar{k} \frac{A_{c,i}}{\Delta x}(T_{i+1} - T_i) + \bar{k} \frac{A_{c,i}}{\Delta x}(T_{i-1} - T_i) + U_w A_{s,i}(T_g - T_i), \tag{13}$$

where t is the time, $m_i = \bar{\rho} V_i$ is the mass of cell "i", $\bar{c}$ is the average specific heat of the storage system, $\bar{k}$ is the average thermal conductivity of storage medium, U_w is the heat transfer coefficient of the wall, and T_g is the average ground temperature, which depends on several parameters such as the ground thermal conductivity, the TES geometry, the TES envelope heat transfer coefficient, the groundwater flow. In order to have an accurate estimate of the ground temperature distribution around the pit, one should solve the heat diffusion equation in the ground, at least in two dimensions, with appropriate boundary conditions (see, for instance, Ref. [32]). In the present work, a simplified approach has been considered, namely, following the results of the calibrated simulation of Tosatto et al. [32], a constant value of $T_g = 55$ °C has been assumed. The first and the second terms of Eq. (13) represent the thermal energy fluxes associated with mass transport. The stratification of the fluid is mainly governed by the thermal conduction effects (third and fourth terms on the right-hand side). The last term models the heat loss through the external surface of each cell. Fig. 7 reports the corresponding diagram for the energy balance of the generic node i. The averaged quantities in Eq. (13) have been computed as

$$\bar{\rho} = \epsilon(\rho_f) + (1 - \epsilon)(\rho_s),$$

Table 2
Data for TES system simulation.

Parameter	Unit	Value
Fluid specific heat, c_f	J/(kg K)	4186
Fluid density, ρ_f	kg/m^3	985
Fluid thermal conductivity, k_f	W/(m K)	0.58
Solid specific heat, c_s	J/(kg K)	840
Solid density, ρ_s	kg/m^3	1840
Solid thermal conductivity, k_s	W/(m K)	0.36
Porosity, ϵ	–	0.4

$$\bar{c} = \epsilon(c_f) + (1 - \epsilon)(c_s), \qquad \bar{k} = \epsilon k_f + (1 - \epsilon)k_s, \tag{14}$$

where ϵ is the porosity of the dual-media storage system, and the subscripts f and s indicate the fluid and the solid material, respectively.

A grid-refinement study indicates that using a number of cells equal to $N = 5$ provides a grid-independent distribution of the temperature inside the tank. Moreover, a time increment equal to $\Delta t = 1$ h is sufficient to obtain a time evolution independent of the time step. In the present work, a porosity $\epsilon = 0.4$ has been considered. The data for the TES model are reported in Table 2.

A MATLAB code has been developed to implement all the component models described in the present section to obtain a time-dependent simulation of the entire plant. The developed code is based on a finite-difference discretization of the governing equations in time and in space (for the one-dimensional model of the heat exchanger and of the thermal storage system).

4. Economic model

The present section provides the details of the assumptions and of the economic model adopted to estimate the cost of the components of the considered plant.

A cost of 250 Euro/m^2 for the installed solar collectors has been estimated. The cost of the TES is usually related to its volume; in the present work, the following cost correlation for the dual-media pit-TES has been employed, obtained by a regression of the data provided in [44],

$$C^{TES} = 4435\, V_{WE}^{-0.406}\ [\text{Euro/m}^3], \tag{15}$$

where V_{WE} is the water equivalent storage volume, namely, the corresponding water volume to store the same amount of heat. C^{TES} is the cost (Euro) per unit storage volume of water equivalent. Experiences carried out in demonstration plants indicate cost reduction by increasing the storage volume in large-scale solar applications.

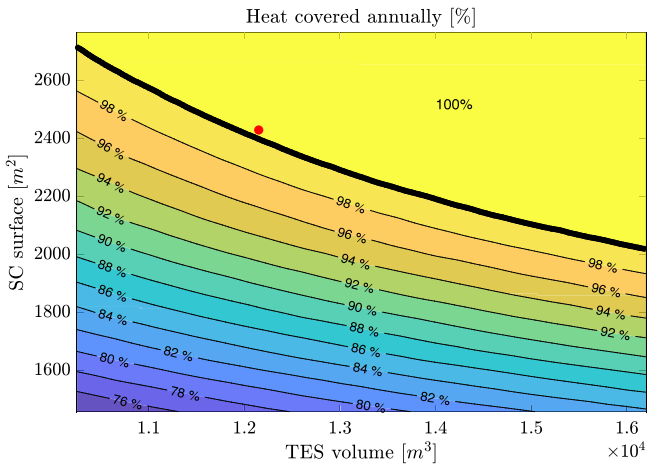

Fig. 8. Heat demand covered by the solar plant: sensitivity analysis. The red circle indicates the chosen design point.

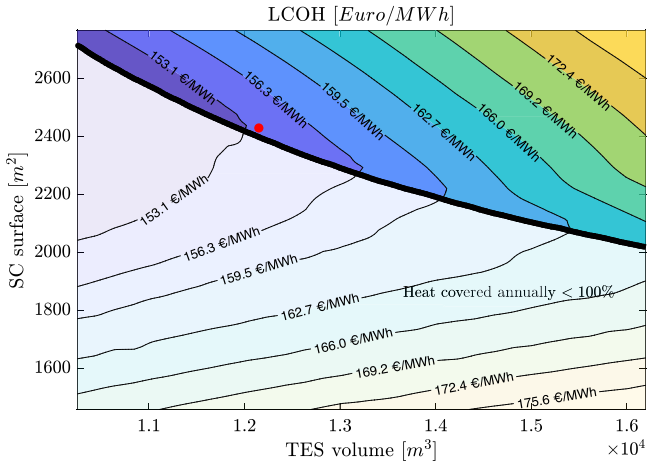

Fig. 9. Levelized cost of heat: sensitivity analysis. The red circle indicates the chosen design point. The gray region represents the points where the system cannot satisfy the total heat demand.

The cost of the heat exchanger is estimated using the following recently developed correlation [40],

$$C_{HEX} = a + b\,A\,[\text{Euro}], \tag{16}$$

with $a = 206$, $b = 336$; the cost is expressed in Euro and A is the surface area in m^2. The costs of pipes and pumps have been considered to be included in the above correlations.

Economic indicators, such as the levelized cost of heat ($LCoH$) and the pay-back time (PBT) are relevant for investment decisions. These indicators depend heavily on the assumptions, e.g., the gas prices and the load profile. The LCoH is defined as:

$$LCoH = \frac{\text{Total cost over lifetime of the plant}}{\text{Total energy delivered over lifetime by the plant}} = \frac{TCP}{TED}, \tag{17}$$

with,

$$TCP = C_c + \sum_{t=1}^{n} \frac{C_{M,t} + C_{O,t}}{(1+r)^t} \tag{18}$$

and

$$TED = \sum_{t=1}^{n} \frac{E_t}{(1+r)^t}, \tag{19}$$

where C_c is the capital cost; $C_{M,t}$ and $C_{O,t}$ are the maintenance and operational costs for year t, respectively; E_t is the energy production in year t; r is the discount rate.

The lifetime of the system has been set to 25 years with a discount rate of 5%. Maintenance costs were assumed to be equal to 1% of the capital cost per year. Operational costs were assumed to be equal to 1% of the capital cost per year increased by the cost of electricity to drive the pumps (0.27 Euro/kWh). The required circulating pumps power was estimated on the basis of the (maximum) mass flow and suitable pressure drops in the piping in the following way: (1) SC pumps: 12 kW; (2) HEX pumps: 2 kW; (3) GH pumps: 20 kW. Regulation of the operating point was performed by varying the speed.

In the standard plant, natural gas is employed to generate the heat load required by the greenhouse using a gas boiler. In order to evaluate the pay-back time of the solar plant, a comparison between the considered solar plant with STES and the standard gas-boiler plant satisfying all the heat demand of the greenhouse is carried on. Therefore, the cost of the natural gas and of the standard gas boiler employed in the greenhouse is needed. Concerning the cost of natural gas for industrial consumers, the database of the "Italian Regulatory Authority for Energy, Networks and Environment" was used, which fix the average final cost of gas to 0.65 Euro/Nm^3 with reference to the year 2020. The cost of the gas boiler is estimated by the following correlation:

$$C_{Bo} = 690\,[\text{Euro/kW}]. \tag{20}$$

Therefore, a boiler of 500 kW, which is actually employed in the greenhouse for satisfying all the heat demand, has an estimated capital cost of 345 kEuro.

5. Results

In the present section, firstly, the results of the thermo-economic analysis are discussed and an optimal operation point for the plant is selected. Then, a detailed analysis of the thermodynamic behavior of the system at the optimal condition is provided.

5.1. Thermo-economic analysis

In order to find suitable values for the area of the solar collector field, A_{SC}, and of the volume of the TES, V_{TES}, a sensitivity analysis of the covered heat load, LCoH and pay-back time for the considered solar plant is provided in the present section. The estimated percentage of the covered annual heating demand is given in Fig. 8 as a function of A_{SC} and V_{TES}, whereas Fig. 9 shows the LCoH. Fig. 8 shows that there is a large region in which the solar plant can provide all the thermal energy requested by the greenhouse. Moreover, Figs. 9 and 10 show that, in such a region, a minimum-cost area exists. In this area, the design point of the plant is selected, namely the point with A_{SC} = 2430 m^2 and V_{TES} = 12150 m^3 (corresponding to a cylinder with radius R_{TES} = 27.81 m and height h_{TES} = 5 m), which guarantees a satisfactory temperature stratification in the TES (as will be shown later). Such a design point corresponds to an estimated LCoH of 153.3 Euro/MWh. It is noteworthy that the total area required by the SC depends on the number of rows of SC panels and on distance between each row necessary to avoid the shadowing effect. At the considered latitudes, the percentage of area occupied by the solar collectors is about 50%, so that the total area required for the SC is about equal to 5000 m^2. From the results of the economic analysis, it can be seen that the annual saving using the proposed energy plant is about 42.03 kEuro, which, compared to an initial cost of about 1430 kEuro, allows a pay-back time of about 29 years for a gas rate of about 0.65 Euro/Nm^3 without considering subsidies and carbon tax (see Fig. 10). For a higher gas price of about 1.30 Euro/Nm^3, the pay-back time estimate would be reduced to about 9 years.

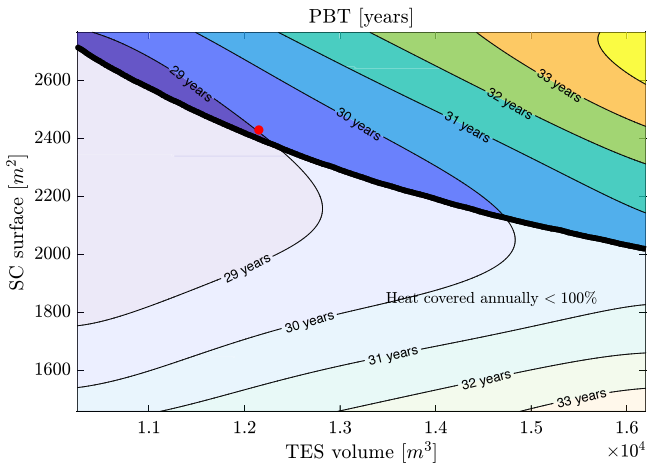

Fig. 10. Pay-back time: sensitivity analysis. The red circle indicates the chosen design point. The gray region represents the points where the system cannot satisfy the total heat demand.

5.2. Thermo-dynamic analysis

Using the values of A_{SC} and V_{TES} of the previous section, the thermal energy supplied by the solar system was calculated on an hourly basis for one year. Firstly, this solar energy production has been compared with the hourly heat demand required by the greenhouse without using the seasonal TES. The results show that, although the annual energy production provided by the solar plant is higher than that required by the greenhouse, due to the mismatch between energy production and demand, only 12% of the required energy can be supplied by the solar plant. Therefore, it is clear that a seasonal thermal energy storage system is mandatory for this application.

Fig. 11 shows the temperature distribution inside the TES during the one-year period of simulation. The simulation has been iterated over a period of one year until achieving periodicity in time, eliminating the influence of an arbitrary initial condition on the temperature of the STES system. It appears that a good temperature stratification is achieved with the chosen configuration. Fig. 12 provides the thermal energy stored in the STES system during the period of observation. At the conditions of maximum stored energy, in November, the maximum temperature inside the STES is about 90 °C, whereas the minimum temperature is about 40 °C in April. Heating supplied by the solar system decreases throughout the winter months so that the energy stored in the STES reduces and, during the month of March, achieves its minimum. From that moment on, during the spring and the summer (from April to September), the energy stored in the STES increases, as shown in Fig. 12. Therefore, by choosing a sufficiently large STES volume, as the one considered here, the most critical point in March can be overcome and all the required thermal load can be provided by the solar energy due to the action of the STES.

Fig. 13 provides the inlet and outlet temperatures of the solar collector and of the TES during one day in April. When the solar radiation is insufficient to rise the temperature of the water, the solar collector pumps are switched off, and the collector inlet and outlet temperatures are equal. The SC starts working at about 8 a. m. and stops at about 5 p. m. One can observe that the maximum temperature rises through the solar collector is close to 15 °C. It appears that, during the selected day, the maximum and minimum temperatures of the STES are quasi invariant. Fig. 14 provides the inlet and outlet temperatures of the solar collector and of the TES during one day in November. In this case, the SC starts working at about 10 a. m. and stops at about 2 p. m., and the maximum temperature rise through the solar collector is close to 10 °C. Therefore, a smaller portion of solar energy can be harvested with respect to the day of April. Also in this case, due to the high thermal inertia, one cannot notice a variation in the temperature inside the storage system.

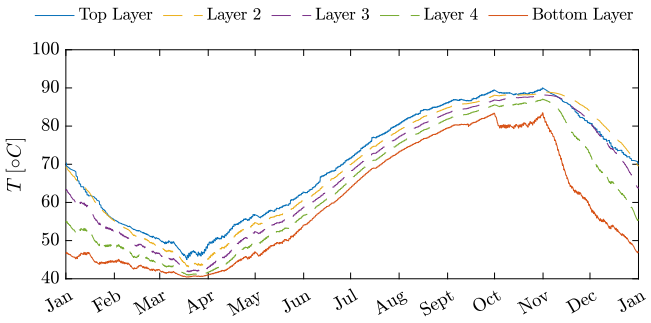

Fig. 11. Temperature distribution in the STES during one year.

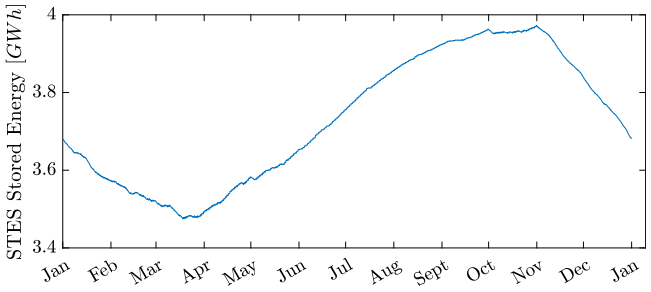

Fig. 12. Thermal energy stored in the STES system.

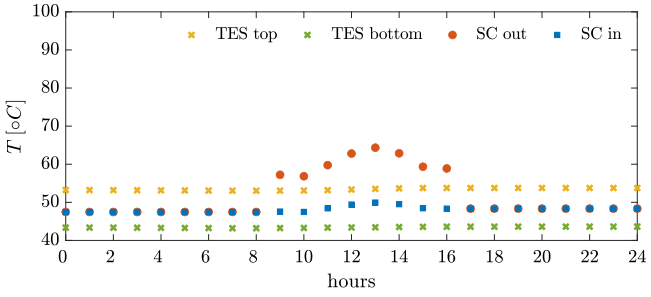

Fig. 13. Temperature distribution during one day of April: inlet and outlet of solar collector and STES.

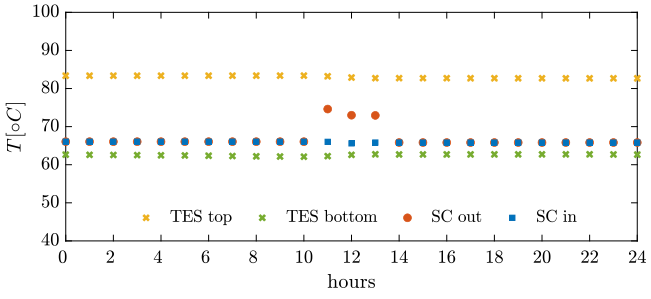

Fig. 14. Temperature distribution during one day of November: inlet and outlet of solar collector and STES.

The analysis is completed by evaluating the environmental impact of the proposed solar plant based on CO_2 emissions. The environmental impact of the standard gas-boiler plant is compared with that of the solar plant. Estimating a production of 0.185 kg of CO_2 per kWh of heat obtained by natural gas and of 0.3 kg of CO_2 per kWh of electric energy to drive the pumps, the simulation indicates a reduction of CO_2 emissions equal to 147.5 tons/year using the considered solar

plant (the emissions of the standard gas-boiler plant were estimated in 149.6 tons/year).

The results obtained for the proposed pit storage technology demonstrate that this solution is competitive with the storage system of Semple et al. [6], who instead employed a solar collector field in conjunction with a small buffer storage tank and a borehole thermal energy storage system for a greenhouse. Mohebi et al. (2023) have recently proposed a study for a greenhouse with a surface similar to the one considered in the present work. They presented an optimization strategy for a hybrid gas-solar energy system with long-term heat storage that satisfies the heating demand of the greenhouse while minimizing the annual cost. This approach optimizes sizing and hourly-based operation of the energy system for the time horizon of a whole year to take seasonal characteristics into account. Mohebi and Roshandel [34] aim at minimizing the annual cost of the plant by controlling the solar collector field area, the size of the gas boiler and the storage system. This gives as result a relatively small storage capacity (457 MWh), about one order of magnitude smaller compared to the result obtained in the present analysis; with a larger solar collector area equal to 65.4% of the greenhouse area, and with a 155.8 kW boiler. In this way, solar energy could cover 96.7% of the thermal energy request of the greenhouse. Instead, in the present case, at the considered latitudes, using a solar collector field with an area equal to 22.5% of the greenhouse, we can avoid the use of the boiler and satisfy the complete energy request by the solar energy, nearly completely canceling the production of carbon dioxide. It is noteworthy that, such a value of the percentage of the solar collector area with respect to the greenhouse area is in the "optimal" range indicated by Mohebi and Roshandel [34], namely, 10.6%–65.4%. Moreover, it is very close to the value found by Xu et al. [45] who studied experimentally a smaller greenhouse of 2304 m^2 with a solar collector field of 500 m^2 (21,7%) for which all of the heat required by the greenhouse was supplied by solar energy. Therefore, these data demonstrate that the proposed methodology to estimate the size of the solar collector field and of the volume of the TES is effective to design a solar plant capable of fully satisfying the thermal energy request of the greenhouse, at least at the considered latitudes, by using a dual-media pit energy storage system. The choice of the dual-media TES system is a peculiar design choice of the proposed plant, which would allow to save surface soil by putting the TES under the greenhouse and to maintain the temperature stratification in the TES. The present thermo-economic analysis, based on recent real data, indicates that the considered low-cost DM-SHTES system shows a combination of pay-back time and covered heat demand which renders the proposed solution very attractive in general for greenhouse heat supply with respect to other solar energy systems with energy storage, such as those discussed in the recent review of Gorjian et al. [8].

6. Conclusions

This paper provides a numerical study of a thermal solar plant using a seasonal dual-media sensible heat thermal energy storage (DM-SHTES) system for a greenhouse located in the South of Italy. The aim of this work is to assess the technical and economic performance of a low-cost seasonal pit storage system, made of gravel and water, which can be placed under the greenhouse to save surface. The greenhouse occupies an area of 10800 m^2 area and has an overall annual thermal energy demand equal to 809 MWh. The DM-SHTES system is coupled with a thermal solar field, made of flat plate solar collectors, designed to cover the total annual heating demand of the greenhouse. The assessment is carried on by a thermo-economic analysis of the overall plant based on real thermo-dynamic data measured on the field, elaborated through a MATLAB software developed by the authors. The study provides the transient analysis of the charging and discharging phases during one year of operation on the base of the hourly heating demand data of the greenhouse and on real hourly weather data. A model of the entire plant is developed including the greenhouse, the solar collector field, the DM-SHTES, and the heat exchanger. The time-dependent simulation of the system is performed over a one-year time scale and an assessment of the economic return and environmental impact of the plant is provided. A sensitivity analysis for the fraction of covered heat demand, for the levelized cost of heat (LCoH) and for the pay-back time has been provided. These quantities have been computed as a function of the area of the solar collector, A_{SC}, and of the volume of the DM-SHTES, V_{TES}. The analysis shows that a range of values of (A_{SC}, V_{TES}) for which the total heat demand is covered exists; moreover, in such a range, there is a minimum-LCoH area. In this area, the design point of the plant is selected, having A_{SC} = 2430 m^2 and V_{TES} = 12150 m^3 corresponding to an LCoH equal to 153.3 Euro/MWh. The area of the solar collector is equal to 22.5% of the surface of the greenhouse, in agreement with previous studies available in the literature. Moreover, the simulation indicates a reduction of CO_2 emissions equal to 147.5 tons/year with respect to using a standard gas boiler. A detailed analysis of the unsteady thermodynamic parameters characterizing the operation of all components of the plant, and in particular, of the solar collector and of the DM-SHTES has been provided. This analysis has shown that: (i) the system can sustain, during all the observation time, a good temperature stratification in the DM-SHTES, guaranteeing the complete supply of the heat demand; (ii) the low-cost thermal-energy pit storage technology for heat supply to greenhouses is a mature solution and it can be economically sustainable under the actual costs of natural gas. The value of the estimated levelized cost of heat is in agreement with other studies available in the literature and can be considered feasible but rather high, corresponding to a pay-back time of about 29 years. This result has been obtained in absence of subsidies and carbon tax. The results of the present analysis and the developed methodology can be extended to district heating systems, considering larger scale plants. Future work will be focused on improving the accuracy of the methodology by adopting a two- or three-dimensional modeling of the pit thermal energy storage system, based on a computational fluid dynamic approach, including the simulation of the heat diffusion in the surrounding ground.

Nomenclature

A area
c specific heat
C cost
d diffusive fraction
E internal energy
h heat transfer coefficient; entalpy
I solar irradiance
k thermal conductivity
k_t clearness index
$\dot{m}$ mass flow
$\dot{Q}$ heat power
r discount rate
R radius
s thickness
T temperature
U heat transfer coefficient
V volume
x space coordinate
z solar zenith angle

Greek letters

ϵ porosity
η efficiency
ρ density

Subscripts

c capital
ch charge
dis discharge
f fluid

g ground
i cell index
M maintenance
O operational
si sink
so source
s solid material
t time index

Abbreviations

DM dual media
GH greenhouse
GHG green house gas
HEX heat exchanger
HTC heat transfer coefficient
IEA International Energy Agency
LCoH levelized cost of heat
PBT pay-back time
PV photovoltaic
SC solar collector
TCP total cost over lifetime of the plant
TED total energy delivered over lifetime
SH sensible heat
STES seasonal thermal energy storage
TES thermal energy storage

CRediT authorship contribution statement

A. Tafuni: Data curation, Formal analysis, Methodology, Investigation, Writing – original draft. **A. Giannotta:** Conceptualization, Methodology, Validation, Formal analysis, Investigation, Writing – review & editing. **M. Mersch:** Methodology, Validation. **A.M. Pantaleo:** Conceptualization, Investigation, Writing – original draft, Writing – review & editing, Supervision. **R. Amirante:** Conceptualization, Investigation, Writing – review & editing. **C.N. Markides:** Methodology, Investigation, Supervision. **P. De Palma:** Conceptualization, Methodology, Investigation, Writing – original draft, Writing – review & editing, Supervision.

Declaration of competing interest

The authors declare that they have no known competing financial interests or personal relationships that could have appeared to influence the work reported in this paper.

Data availability

The authors do not have permission to share data.

Acknowledgments

The first author has been supported by a Ph. D. fellowship by Ministero dell'Università e della Ricerca (Project: PON Ricerca e Innovazione 2014–2020).

References

[1] IEA. World energy outlook. Technical report, International Energy Agency; 2022.
[2] IEA. Global energy review 2021. Assessing the effects of economic recoveries on global energy demand and CO2 emissions in 2021. Technical report, International Energy Agency; 2021.
[3] IEA. Renewables 2022. Analysis and forecast to 2027. Technical report, International Energy Agency; 2019.
[4] IEA. Heating. Technical report, International Energy Agency; 2021, https://www.iea.org/reports/heating.
[5] IEA. Net zero by 2050. A roadmap for the global energy sector. Technical report, International Energy Agency; 2021.
[6] Semple L, Carriveau R, Ting DS-K. A techno-economic analysis of seasonal thermal energy storage for greenhouse applications. Energy Build 2017;154:175–87.
[7] Sturm B, Maier M, Royapoor M, Joyce S. Dependency of production planning on availability of thermal energy in commercial greenhouses-a case study in Germany. Appl Therm Eng 2014;71:239–47.
[8] Gorjian S, Calise F, Kant K, Ahamed MS, Copertaro B, Najafi G, et al. A review on opportunities for implementation of solar energy technologies in agricultural greenhouses. J Clean Prod 2021;285:124807.
[9] Acosta-Silva YdJ, Torres-Pacheco I, Matsumoto Y, Toledano-Ayala M, Soto-Zarazúa GM, Zelaya-Angel O, et al. Applications of solar and wind renewable energy in agriculture: A review. Sci Progress 2019;102:127–40.
[10] Mirzamohammadi S, Jabarzadeh A, Shahrabi MS. Long-term planning of supplying energy for greenhouses using renewable resources under uncertainty. J Clean Prod 2020;264:121611.
[11] Mekhilef S, Saidur R, Safari A. A review on solar energy use in industries. Renew Sustain Energy Rev 2021;15:1777–90.
[12] Gorjian S, Ebadi H, Najafi G, Singh F. Recent advances in net-zero energy greenhouses and adapted thermal energy storage systems. Sustain Energy Technol Assess 2021;43:100940.
[13] Gorjian S, Tavakkoli Hashjin T, Ghobadian B, Banakar A. A thermal performance evaluation of a medium-temperature point-focus solar collector using local weather data and artificial neural networks. Int J Green Energy 2015;12:493–505.
[14] Ketabchi F, Gorjian S, Sabzehparvar S, Shadram Z, Ghoreishi MS, Rahimzadeh H. Experimental performance evaluation of a modified solar still integrated with a cooling system and external flat-plate reflectors. Sol Energy 2019;187:137–46.
[15] Gorjian S, Ebadi H, Calise F, Shukla A, Ingrao C. A review on recent advancements in performance enhancement techniques for low-temperature solar collectors. Energy Convers Manage 2020;222:113246.
[16] Ntinas GK, Fragos VP, Nikita-Martzopoulou C. Thermal analysis of a hybrid solar energy saving system inside a greenhouse. Energy Convers Manage 2014;81:428–39.
[17] Ding Z, Wu W, Leung M. Advanced/hybrid thermal energy storage technology: Material, cycle, system and perspective. Renew Sustain Energy Rev 2021;145:111088.
[18] Hasnain S. Review on sustainable thermal energy storage technologies, part I: Heat storage materials and techniques. Energy Convers Manage 1998;39:1127–38.
[19] Gourdo L, Fatnassi H, Tskatine R, Wifaya A, Demrati H, Aharoune A, et al. Solar energy storing rock-bed to heat an agricultural greenhouse. Energy 2019;169:206–12.
[20] Gourdo L, Bazgaou A, Ezzaeri K, Tskatine R, Wifaya A, Demrati H, et al. Heating of an agricultural greenhouse by a reservoir filled with rocks. J Mater Environ Sci 2018;9:1193–9.
[21] Danehkar S, Yousefi H. A comprehensive overview on water-based energy storage systems for solar applications. Energy Rep 2022;8:8777–97.
[22] Vadiee A, Martin V. Thermal energy storage strategies for effective closed greenhouse design. Appl Energy 2013;109:337–43.
[23] Paksoy HÖ, Beyhan B. Thermal energy storage (TES) systems for greenhouse technology. In: Woodhead publishing series in energy, advances in thermal energy storage systems, Woodhead Publishing; 2015, p. 533–48.
[24] Attar I, Farhat A. Efficiency evaluation of a solar water heating system applied to the greenhouse climate. Sol Energy 2015;119:212–24.
[25] Lu W, Zhang Y, Fang H, Ke X, Yang Q. Modelling and experimental verification of the thermal performance of an active solar heat storage-release system in a Chinese solar greenhouse. Biosyst Eng 2017;160:12–24.
[26] Wei B, Guo S, Wang J, Li J, Wang J. Thermal performance of single span greenhouses with removable back walls. Biosyst Eng 2015;141:48–57.
[27] Velraj R. Sensible heat storage for solar heating and cooling systems. In: Advances in solar heating and cooling, Elsevier; 2016, p. 399–428.
[28] Alptekin E, Ezan MA. Performance investigations on a sensible heat thermal energy storage tank with a solar collector under variable climatic conditions. Appl Therm Eng 2020;164:114423.
[29] Lugolole R, Mawire A, Okello D, Lentswe KA, Nyeinga K, Shobo AB. Experimental analyses of sensible heat thermal energy storage systems during discharging. Sustain Energy Technol Assess 2019;35:117–30.
[30] Schmidt T, Mangold D, Muller-Steinhagen H. Central solar heating plants with seasonal storage in Germany. Sol Energy 2020;76:165–74.
[31] Kim D-W, Kim MH, Lee D-W. Economic and environmental analysis of solar thermal and seasonal thermal energy storage based on a renewable energy conversion system for greenhouses. Energies 2022;15:6592.
[32] Tosatto A, Dahash A, Ochs F. Simulation-based performance evaluation of large-scale thermal energy storage coupled with heat pump in district heating systems. J Energy Storage 2023;61:106721.
[33] Dahash A, Ochs F, Tosatto A, Streicher W. Toward efficient numerical modeling and analysis of large-scale thermal energy storage for renewable district heating. Appl Energy 2020;279:115840.
[34] Mohebi P, Roshandel R. Optimal design and operation of solar energy system with heat storage for agricultural greenhouse heating. Energy Convers Manag X 2023;18:100353.

[35] Mersch M, Olympios AV, Sapin P, Mac Dowell N, Markides CN. Solar-thermal heating potential in the UK: A techno-economic whole-energy system analysis. In: Proceedings of Ecos 2021 - The 34th international conference on efficiency, cost, optimization, simulation and environmental impact of energy systems. 2021.
[36] Hofmann M, Seckmeyer G. A new model for estimating the diffuse fraction of solar irradiance for photovoltaic system simulations. Energies 2017;10(2, 248):248.
[37] Carpaneto E, Lazzeroni P, Repetto M. Optimal integration of solar energy in a district heating network. Renew Energy 2015;75:714–21.
[38] Maxwell EL. A quasi-physical model for converting hourly global horizontal to direct normal lnsolation. Technical report, (SERI/TR-215-3087). Solar Energy Research Institute, U.S. Department of Energy; 1987.
[39] Ridley B, Boland J, Lauret P. Modelling of diffuse solar fraction with multiple predictors. Renew Energy 2010;35(2):478–83.
[40] Olympios AV, Hoseinpoori P, Mersch M, Pantaleo M, ans Simpson A M, Sapin P, Mac Dowell N, et al. Optimal design of low-temperature heat-pumping technologies and implications to the whole- energy system. In: Proceedings of Ecos 2020 - The 33rd international conference on efficiency, cost, optimization, simulation and environmental impact of energy systems. 2020.
[41] Bogaert R, Böles A. Global performance of a prototype brazed plate heat exchanger in a large Reynolds number range. Exp Heat Transfer 1995;8:293–311.
[42] Chisholm D, Wanniarachchi AS. Layout of plate heat exchangers. In: ASME/JSME thermal engineering joint conference, 17-22 march. Reno, NV; 1991.
[43] Fan J, Huang J, Chatzidiakos A, Furbo S. Experimental and theoretic investigations of thermal behavior of a seasonal water pit heat storage. In: Solar world congress 2017. Abu Dhabi, United Arab Emirates; 2017.
[44] Yang T, Liu W, Kramer GJ, Sun Q. Seasonal thermal energy storage: A techno-economic literature review. Renew Sustain Energy Rev 2021;139:110732.
[45] Xu J, Li Y, Wang RZ, Liu W. Performance investigation of a solar heating system with underground seasonal energy storage for greenhouse application. Energy 2014;67:63–73.